

1 **American Mineralogist Manuscript 5682 Revision 1**
2 **Yangite, $\text{PbMnSi}_3\text{O}_8 \cdot \text{H}_2\text{O}$, a new mineral species with double**
3 **wollastonite silicate chains, from the Kombat mine, Namibia**

4
5 Robert T. Downs¹, William W. Pinch², Richard M. Thompson^{3*}, Stanley H. Evans¹, and
6 Lauren Megaw¹

7 ¹Department of Geosciences, University of Arizona, 1040 E. 4th Street, Tucson, Arizona 85721, U.S.A.

8 ²19 Stonebridge Lane, Pittsford, New York 14534, U.S.A.

9 ³School of Information, University of Arizona, 1103 E. 2nd Street, Tucson, Arizona 85721, U.S.A.

10 *Corresponding author: rmthomps@email.arizona.edu

11 **Abstract**

12 A new chain-silicate mineral species, yangite, ideally $\text{PbMnSi}_3\text{O}_8 \cdot \text{H}_2\text{O}$, has been
13 found on a specimen from the Kombat mine, Otavi Valley, Namibia. Associated minerals
14 are melanotekite and rhodochrosite. Yangite is colorless to pale brown in transmitted
15 light, transparent with white streak and vitreous luster. Broken pieces of yangite crystals
16 are bladed or platy, and elongated along [010]. It is sectile with a Mohs hardness of ~5;
17 cleavage is perfect on {101} and no twinning or parting was observed. The measured and
18 calculated densities are 4.14(3) and 4.16 g/cm³, respectively. Optically, yangite is biaxial
19 (-), with $n_\alpha = 1.690(1)$, $n_\beta = 1.699(1)$, $n_\gamma = 1.705(1)$, $Y = b$, $Z \wedge c = 11^\circ$ and $2V_{\text{meas}} =$
20 $77(2)^\circ$. It is insoluble in water, acetone, and hydrochloric acid. An electron microprobe
21 analysis demonstrated that the sample was relatively pure, yielding the empirical formula
22 (with calculated H₂O) $\text{Pb}_{1.00}\text{Mn}^{2+}_{1.00}\text{Si}_{3.00}\text{O}_8 \cdot \text{H}_2\text{O}$.

23 Yangite is triclinic and exhibits space group symmetry *P*-1 with unit-cell
24 parameters $a = 9.6015(9)$, $b = 7.2712(7)$, $c = 7.9833(8)$ Å, $\alpha = 105.910(4)$, $\beta = 118.229(4)$,
25 $\gamma = 109.935(5)^\circ$, and $V = 392.69(7)$ Å³. Its crystal structure is based on a skeleton of double
26 wollastonite SiO₄ tetrahedral chains oriented parallel to [010] and interlinked with

27 ribbons of Mn- and Pb-polyhedra. Yangite represents the first chain silicate with two-
28 connected double chains and possesses all of the structural features of a hypothetical
29 triclinic $\text{Ca}_2\text{Si}_3\text{O}_8 \cdot 2\text{H}_2\text{O}$ phase proposed by Merlini and Bonaccorsi (2008) as a
30 derivative of the okenite structure. The difference in the H_2O component between the
31 hypothetical phase and yangite likely is a consequence of the larger Pb^{2+} with its lone-
32 pair electrons in yangite replacing the smaller Ca^{2+} in the hypothetical phase.

33 **Key words:** yangite, chain silicate, wollastonite chains, crystal structure, X-ray
34 diffraction, Raman spectra

35 **Introduction**

36 A new mineral species and new type of chain silicate, ideal formula
37 $\text{PbMnSi}_3\text{O}_8 \cdot \text{H}_2\text{O}$, has been found on a specimen from the Kombat mine, Otavi Valley,
38 Namibia. It is named yangite to honor the contributions of Dr. Hexiong Yang,
39 Department of Geosciences, University of Arizona, to the fields of chain silicates in
40 particular and mineralogy in general, and his stewardship of the RRUFF project's
41 (<http://rruff.info>) ambitious attempt to characterize the known minerals chemically,
42 structurally, and spectrographically. The new mineral and its name have been approved
43 by the Commission on New Minerals and Nomenclature and Classification (CNMNC) of
44 the International Mineralogical Association (IMA2012-052). Part of the cotype sample
45 has been deposited at the University of Arizona Mineral Museum (Catalogue # 19341),
46 the RRUFF Project (deposition # R090031), and the Smithsonian Institution, Washington
47 DC, USA (catalogue number 175983). This paper describes the physical and chemical
48 properties of yangite, and its single-crystal X-ray diffraction and Raman spectroscopic
49 data.

50 **Sample Description and Experimental Methods**

51 *Occurrence, physical and chemical properties, and Raman spectra*

52 Yangite was found on a single specimen from the Kombat mine, Namibia, in the
53 collection of the late John Innes (Figure 1). Innes was a senior mineralogist in the

54 employ of the Tsumeb Corporation and has been honored for his studies of the geology
55 and mineralogy of the Tsumeb and Kombat mines with a mineral name, johninnesite (c.f.
56 Innes and Chaplin 1986). He gave the piece to co-author Bill Pinch with the recognition
57 that it was unique.

58 A brief summary of relevant geological information follows, taken from a detailed
59 presentation of the geology of the Kombat Mine authored by Innes and Chaplin (1986).
60 The Kombat mine, located in the Otavi Valley, 37 km east of Otavi and 49 km south of
61 Tsumeb, is in a sequence of weakly metamorphosed, thin to massive bedded, shallow-
62 water dolostones of the Upper Proterozoic Hüttenberg Formation. Six discrete bodies of
63 brecciated, hydrothermally deposited massive sulphide ores are present along a
64 disconformity separating dolostone from younger slate. Elements that occur in economic
65 concentrations include copper, lead, and silver. Iron and manganese are abundant. Other
66 elements found at Kombat in significant concentrations include zinc, barium, arsenic,
67 chromium, molybdenum, chlorine, and germanium.

68 Yangite occurs in an epithermal association, one of seven described ore types.
69 The others are massive and semi-massive sulphides, mineralized net-vein fracture
70 systems, galena-rich alteration breccias, a pyrite-sericite association, an iron-manganese
71 oxide/silicate association, and mineralized fracture fillings. The epithermal association
72 postdates main mineralization and consists of vuggy veins of calcite, quartz, and
73 chalcopyrite; narrow veins of galena, rhodochrosite, helvite, and barite; and a rare
74 assemblage in the Kombat Central ore body of manganite-nambulite-serandite-barite-
75 cahnite-brushite-kentrolite-calcite-gypsum. Yangite presumably comes from the narrow
76 rhodochrosite-bearing veins.

77 Dunn (1991) reviewed rare minerals found in the Kombat Mine, including four
78 Pb-silicates: barysilite, melanotekite, kentrolite, and molybdophyllite. Yangite increases
79 the total of Pb-silicates to five, and is found in a massive assemblage with melanotekite
80 $\text{Pb}_2\text{Fe}^{3+}_2\text{O}_2\text{Si}_2\text{O}_7$ and rhodochrosite MnCO_3 . Figure 1 is a photograph of a spray of

81 yangite in a matrix of black massive melanotekite and brown rhodochrosite. Broken
82 pieces of yangite crystals are bladed or platy, elongated along [010], and up to 12 mm
83 long. No twinning is apparent in any of the samples.

84 The mineral is colorless to pale brown in transmitted light under microscopy,
85 transparent with white streak and vitreous luster. It is sectile and has a Mohs hardness of
86 ~5; cleavage is perfect on {101} and no parting was observed. Fractures are uneven. The
87 measured (by heavy-liquid) and calculated densities are 4.14(3) and 4.16 g/cm³,
88 respectively. Optically, yangite is biaxial (-), with $n_{\alpha} = 1.690(1)$, $n_{\beta} = 1.699(1)$, $n_{\gamma} =$
89 $1.705(1)$, $Y = b$, $Z \wedge c = 10.7^{\circ}$, $2V_{\text{meas}} = 77(2)^{\circ}$, and $2V_{\text{calc}} = 78^{\circ}$. It is insoluble in water,
90 acetone, and hydrochloric acid.

91 The chemical composition of yangite was determined with a CAMECA SX100
92 electron microprobe at 15 kV and 5 nA with a beam diameter of 20 μm . The standards
93 include diopside for Si, rhodonite for Mn, and NBS_K0229 (Pb-glass) for Pb, yielding an
94 average composition (wt.%) (10 points) of SiO₂ 36.59(19), MnO 14.45(11), PbO
95 45.46(41), H₂O 3.66 added on the basis of structural results, resulting in a total of
96 100.16(34). The presence of H₂O in yangite was confirmed by Raman spectroscopic
97 measurements and structure determination (see below). Trace amounts of Fe and Ca were
98 observed from WDS, but they were under the detection limits of the analysis. The
99 resultant chemical formula, calculated on the basis of 9 O atoms (from the structure
100 determination), is Pb_{1.00}Mn_{1.00}Si_{3.00}O₈·H₂O, or simply PbMnSi₃O₈·H₂O.

101 The Raman spectrum of yangite was collected from a randomly oriented crystal
102 on a Thermo Almega microRaman system, using a 532-nm solid-state laser with a
103 thermoelectric cooled CCD detector. The laser is partially polarized with 4 cm⁻¹
104 resolution and a spot size of 1 μm .

105 *X-ray crystallography*

106 Both powder and single-crystal X-ray diffraction data of yangite were collected
107 on a Bruker X8 APEX2 CCD X-ray diffractometer equipped with graphite-

108 monochromatized MoK_α radiation. However, it is difficult to unambiguously index all
109 powder X-ray diffraction peaks due to severe peak overlaps. Table 1 lists the measured
110 powder X-ray diffraction data, along with those calculated from the determined structure
111 using the program XPOW (Downs et al. 1993).

112 Single-crystal X-ray diffraction data for yangite were collected from an
113 untwinned, elongated tabular crystal (0.06 x 0.04 x 0.03 mm) with frame widths of 0.5°
114 in ω and 30 s counting time per frame. All reflections were indexed on the basis of a
115 triclinic unit-cell (Table 2). No satellite or super-lattice reflections were observed. The
116 intensity data were corrected for X-ray absorption using the Bruker program SADABS.
117 The absence of any systematic absences of reflections suggest possible space groups $P1$
118 or $P-1$. The crystal structure was solved and refined using SHELX97 (Sheldrick 2008)
119 based on the space group $P-1$ because it produced the better refinement statistics in terms
120 of bond lengths and angles, atomic displacement parameters, and R factors. The positions
121 of all atoms were refined with anisotropic displacement parameters, except for H atoms,
122 which were not located from the difference Fourier maps. Final coordinates and
123 displacement parameters of the atoms in yangite are listed in Table 3 and selected bond-
124 distances in Table 4.

125 Discussion

126 *Crystal structure*

127 The crystal structure of yangite consists of double wollastonite SiO_4 tetrahedral
128 chains running parallel to \mathbf{b} and sharing corners with ribbons of Mn- and Pb-polyhedra
129 (Figure 2a). These double chains are characterized by alternating 4- and 6-membered
130 tetrahedral rings, like those found in okenite, $\text{Ca}_{10}\text{Si}_{18}\text{O}_{46}\cdot 18\text{H}_2\text{O}$ (Figure 2b) (Merlino
131 1983). In okenite, however, layers of parallel double chains stacked along \mathbf{c}^* alternate
132 with sheets of tetrahedra composed of 5- and 8-membered rings. Similar double
133 wollastonite chains have also been found in synthetic compounds (Haile and Wuensch
134 1997, 2000; Radić and Kahlenberg 2001; Radić et al. 2003).

135 There are three distinct tetrahedral Si sites in yangite, Si1, Si2, and Si3, with
136 average Si-O bond distances of 1.622, 1.622, and 1.624 Å, respectively. Among them, the
137 Si3 tetrahedron is the most distorted and the Si2 the least, as measured by tetrahedral
138 angle variance and quadratic elongation (Robinson et al. 1971) (Table 4), but none are
139 unusually distorted.

140 The Mn²⁺ cation is octahedrally coordinated. Bond-valence sums calculated
141 using the parameters given by Brese and O’Keeffe (1991) indicate that Mn is 2+, rather
142 than 3+, and that O9W is H₂O (Table 5). The cation coordination octahedron is relatively
143 undistorted, especially given that one corner is anchored by a water molecule, with an
144 angle variance of 34.06 and a quadratic elongation of 1.01.

145 The bonding topology of yangite was calculated using the procrystal
146 representation of its electron density. Procrystal electron density is computed by
147 summing the contributions of the spherically-averaged electron density of neutral atoms
148 placed at the experimentally determined locations of the atoms in a crystal (c.f. Downs et
149 al. 2002, Downs 2003 for details of the method and evidence of its accuracy and
150 efficacy). Calculations were performed with in-house software using the most accurate
151 available analytical Hartree-Fock wave functions (Koga et al. 1999, Koga et al. 2000,
152 Thakkar and Koga 2003).

153 The results suggest that Pb²⁺ is five-coordinated, with all Pb-O bond distances
154 shorter than 2.770 Å (Table 4). As explained in the companion paper, (Thompson et al.
155 this issue), geometrical constraints in pyroxenoids arising from the nature of the
156 octahedral and tetrahedral chains dictate that at least one *M* site must be very distorted.

157 Procrystal calculations also indicate the presence of a three weak O9W-O bonds
158 and a weak, long O9W-Pb interaction that bridges the channel between the parallel bands
159 of Mn/Pb polyhedra. Interestingly, the computation was performed using an oxygen atom
160 at the location of O9W, i.e. without the protons. It is not possible to determine the nature
161 of these bonds given that the unlocated hydrogen atoms were disregarded in the

162 computation, but it is certainly possible that the Pb^{2+} lone pair is involved in a hydrogen
163 bond with O9W. However, it is not obvious how the hydrogens fit into the structure. A
164 more extensive discussion of this issue is in the companion paper (Thompson et al. this
165 issue).

166 The bulk structure of yangite can be regarded as layers of SiO_4 tetrahedra
167 alternating with those of Mn- and Pb-polyhedra stacked along \mathbf{c}^* (Figure 3). For an
168 analysis of the structural relationships between yangite and other pyroxenoids, see the
169 companion paper, Thompson et al. (this issue).

170 *Raman spectra*

171 There have been numerous Raman spectroscopic studies on materials with
172 wollastonite-like silicate chains (e.g., Mills et al. 2005; Makreski et al. 2006; Wierzbicka-
173 Wieczorek et al. 2010; Can et al. 2011). In particular, Frost et al. (2012) measured the
174 Raman spectra of xonotlite, a mineral with one-connected double wollastonite chains (the
175 *n-connected* terminology describes the number of connecting tetrahedra between chains
176 and is due to Merlino and Bonaccorsi 2008). The Raman spectrum of yangite is displayed
177 in Figure 4, along with the Raman spectra of xonotlite and elpidite taken from the
178 RRUFF Project (R120029 and R060200, respectively) for comparison.

179 Due to extremely strong sample fluorescence, we were unable to improve the
180 spectral quality of yangite above 1500 cm^{-1} . Nonetheless, the broad bands between 3200
181 and 3850 cm^{-1} may be ascribed to the O-H stretching vibrations. The two sharp bands at
182 1015 and 916 cm^{-1} are due to the Si-O stretching vibrations within the SiO_4 groups,
183 whereas the bands between 300 and 900 cm^{-1} are primarily attributable to the O-Si-O and
184 Si-O-Si angle bending vibrations (Dowty 1987; Makreski et al. 2006; Frost et al. 2012).
185 The bands below 320 cm^{-1} are of a complex origin, mostly associated with the rotational
186 and translational modes of SiO_4 tetrahedra, Mn-O and Pb-O interactions.

187

Implications

188 A great number of natural and synthetic phases, mostly hydrous Ca-silicates,
189 display crystal structures characterized by the presence of double wollastonite chains.
190 Merlino and Bonaccorsi (2008) presented a thorough review of such compounds and
191 classified them into three categories based on the number of tetrahedra shared between
192 two single chains: one-, two-, and three-connected chains, exemplified by those in
193 xonotlite, okenite, and elpidite, respectively. However, unlike xonotlite or elpidite,
194 okenite is not a “pure” chain silicate, as its structure consists of both silicate chains and
195 sheets (Merlino 1983). Therefore, yangite represents the first chain silicate with two-
196 connected double chains. Furthermore, the discovery of yangite implies that more Pb-
197 silicate compounds or minerals with the chemical formula $PbMSi_3O_8 \cdot H_2O$ ($M = Fe^{2+}$,
198 Ca^{2+} , Mg^{2+} , and other divalent cations) may be synthesized or found in nature, as
199 substitution between Mn and other divalent cations is rather common in pyroxenoids.

200 By eliminating the silicate tetrahedral sheets in the okenite structure, Merlino and
201 Bonaccorsi (2008) derived a hypothetical structure with the composition $Ca_2Si_3O_8 \cdot 2H_2O$,
202 space group $P-1$, and unit-cell parameters $a = 9.69$, $b = 7.28$, $c = 8.11 \text{ \AA}$, $\alpha = 103.0$, $\beta =$
203 118.5 , $\gamma = 112.1^\circ$ (Table 2). Most remarkably, comparison of yangite and the model
204 structure proposed by Merlino and Bonaccorsi (2008) reveals that, except for the amount
205 of H_2O , this hypothetical phase possesses all of the structural features found in yangite
206 (Table 2, Figure 2). The differences in the H_2O contents and unit-cell parameters between
207 the hypothetical phase and yangite are most likely to result from the substitution of larger
208 Pb^{2+} with its lone-pair electrons for smaller Ca^{2+} .

209 **Acknowledgements**

210 This study was funded by Science Foundation Arizona. We are grateful to Dr.
211 Stefano Merlino for providing us with his unpublished data and Dr. Ajit Thakkar for
212 providing us with his electron wave functions. We also thank Dr. Merlino and two
213 anonymous reviewers, along with Associate Editor Dr. Fernando Colombo, for their
214 comments, which have improved the quality of this manuscript.

215

References Cited

- 216 Brese, N.E. and O’Keeffe, M. (1991) Bond-valence parameters for solids. *Acta*
217 *Crystallographica*, B47, 192-197.
- 218 Can, N., Guinea, J.J.G., Kibar, R., and Cetin, A. (2011) Luminescence and Raman
219 characterization of rhodonite from Turkey. *Spectroscopy Letters*, 44, 566-569.
- 220 Dowty, E. (1987) Vibrational interactions of tetrahedra in silicates glass and crystals: II.
221 Calculations on melilites, pyroxenes, silica polymorphs and feldspars. *Physics and*
222 *Chemistry of Minerals*, 14, 122-138.
- 223 Downs, R.T. (2003) Topology of the pyroxenes as a function of temperature, pressure,
224 and composition as determined from the procrystal electron density. *American*
225 *Mineralogist* 88, 556-566.
- 226 Downs, R.T., Bartelmehs, K.L., Gibbs, G.V. and Boisen, M.B., Jr. (1993) Interactive
227 software for calculating and displaying X-ray or neutron powder diffractometer
228 patterns of crystalline materials. *American Mineralogist*, 78, 1104-1107.
- 229 Downs, R.T., Gibbs, G.V., Boisen, M.B.Jr., and Rosso, K.M. (2002) A comparison of
230 procrystal and ab initio representations of the electron-density distributions of
231 minerals. *Physics and Chemistry of Minerals* 29, 369-385.
- 232 Dunn, P.J. (1991) Rare minerals of the Kombat Mine. *Mineralogical Record*, 22, 421-
233 424.
- 234 Frost, R.L., Mahendran, M., Poologanathan, K., and Xi, F. (2012) Raman spectroscopic
235 study of the mineral xonotlite $\text{Ca}_6\text{Si}_6\text{O}_{17}(\text{OH})_2$ —A component of plaster boards.
236 *Materials Research Bulletin*, 47, 3644-3649.
- 237 Haile, S.M. and Wuensch, B.J. (1997) Comparison of the crystal chemistry of selected
238 $\text{MSi}_6\text{O}_{15}$ -based silicates. *American Mineralogist*, 82, 1141-1149.
- 239 Haile, S.M. and Wuensch, B.J. (2000) Structure, phase transitions and ionic conductivity
240 of $\text{K}_3\text{NdSi}_6\text{O}_{15}\cdot x\text{H}_2\text{O}$. I. $\alpha\text{-K}_3\text{NdSi}_6\text{O}_{15}\cdot 2\text{H}_2\text{O}$ and its polymorphs. *Acta*
241 *Crytallographica*, B56, 335-345.

- 242 Innes, J. and Chaplin, R.C. (1986) Ore bodies of the Kombat Mine, South West
243 Africa/Namibia. in Anhaeusser, C.R. and Maske, S. (Eds.): Mineral Deposits of
244 South Africa, Vol. 1 and 2. Geological Society of South Africa, Johannesburg,
245 Republic of South Africa, pp. 1789-1805.
- 246 Koga, T., Kanayama, K., Watanabe, T., Imai, T., and Thakkar, A.J. (2000) Analytical
247 Hartree-Fock wave functions for the atoms Cs to Lr. Theoretical Chemistry
248 Accounts, 104, 411-413.
- 249 Koga, T., Kanayama, K., Watanabe, T., and Thakkar, A.J. (1999) Analytical Hartree-
250 Fock wave functions subject to cusp and asymptotic constraints: He to Xe, Li⁺ to
251 Cs⁺, H⁺ to I⁻. International Journal of Quantum Chemistry, 71, 491-497.
- 252 Makreski, P., Jovanovski, G., Gajovic, A., Biljan, T., Angelovski, D., Jacimovic, R.
253 (2006) Minerals from Macedonia. XVI. Vibrational spectra of some common
254 appearing pyroxenes and pyroxenoids. Journal of Molecular Structure, 788, 102-
255 114.
- 256 Merlino, S. (1983) Okenite, Ca₁₀Si₁₈O₄₆·18H₂O: the first example of a chain and sheet
257 silicate. American Mineralogist, 68, 614-622.
- 258 Merlino, S. and Bonaccorsi, E. (2008) Double wollastonite chains:
259 topological/conformational varieties, polytypic forms, isotypic compounds.
260 Zeitschrift für Kristallographie 223, 85-97.
- 261 Mills, S.J., Ray L. Frost, R.L., Klopogge, J.T., and Weier, M.L. (2005) Raman
262 spectroscopy of the mineral rhodonite. Spectrochimica Acta, 62, 171-175.
- 263 Radić, S. and Kahlenberg, V. (2001) Single crystal structure investigation of twinned
264 NaKSi₂O₅ --- a novel single layer silicate. Solid State Sciences, 3, 659-667.
- 265 Radić, S., Kahlenberg, V., and Schmidt, B.C. (2003) High-pressure mixed alkali disilicates
266 in the system Na_{2-x}K_xSi₂O₅: hydrothermal synthesis and crystal structures of
267 NaKSi₂O₅-II and Na_{0.67}K_{1.33}Si₂O₅. Zeitschrift für Kristallographie 218, 413-420.
- 268 Robinson, K., Gibbs, G.V., and Ribbe, P.H. (1971) Quadratic elongation, a quantitative

- 269 measure of distortion in coordination polyhedra. *Science*, 172, 567–570.
- 270 Sheldrick, G. M. (2008) A short history of *SHELX*. *Acta Crystallographica*, A64, 112-
- 271 122.
- 272 Thakkar, A.J. and Koga, T. (2003) Analytic Hartree-Fock wave functions for atoms and
- 273 ions. *Fundamental World of Quantum Chemistry: A tribute to the memory of Per-*
- 274 *Olov Löwdin*, Vol. I, E.J. Brändas and E.S. Kryachko (eds), 587-599.
- 275 Thompson, R.T., Yang, H., and Downs, R.T. (2016) Ideal Wollastonite and the
- 276 Relationship Between the Pyroxenoids and Pyroxenes. *American Mineralogist* x,
- 277 y-z.
- 278 Wierzbicka-Wieczorek, M., Kolotsch, U., Nasdala, L., Tillmanns, E. (2010)
- 279 $K_{2.9}Rb_{0.1}ErSi_3O_9$: a novel, non-centrosymmetric chain silicate and its crystal
- 280 structure. *Mineralogical Magazine*, 74, 979-990.

281

282 **List of Figure Captions**

- 283 Figure 1. (a) Rock samples on which yangite crystals are found; (b) A microscopic
- 284 view of yangite, associated with dark brown melanotekite.
- 285 Figure 2. (a) Crystal structure of yangite, showing the double chains of SiO_4 tetrahedra
- 286 and ribbons of Mn- and Pb-polyhedra. (b) A portion of the okenite structure
- 287 (Merlino 1983), showing its similarity to the yangite structure. The spheres in
- 288 both figures represent H_2O .
- 289 Figure 3. Crystal structure of yangite. The large and small spheres represent Pb and H_2O
- 290 groups, respectively. The octahedra and tetrahedra represent MnO_6 and SiO_4
- 291 groups, respectively. For clarity, no chemical bonds are drawn for Pb.
- 292 Figure 4. Raman spectrum of yangite, along with the Raman spectra of xonoltite and
- 293 elpidite for comparison. The spectra are shown with vertical offset for more
- 294 clarity.

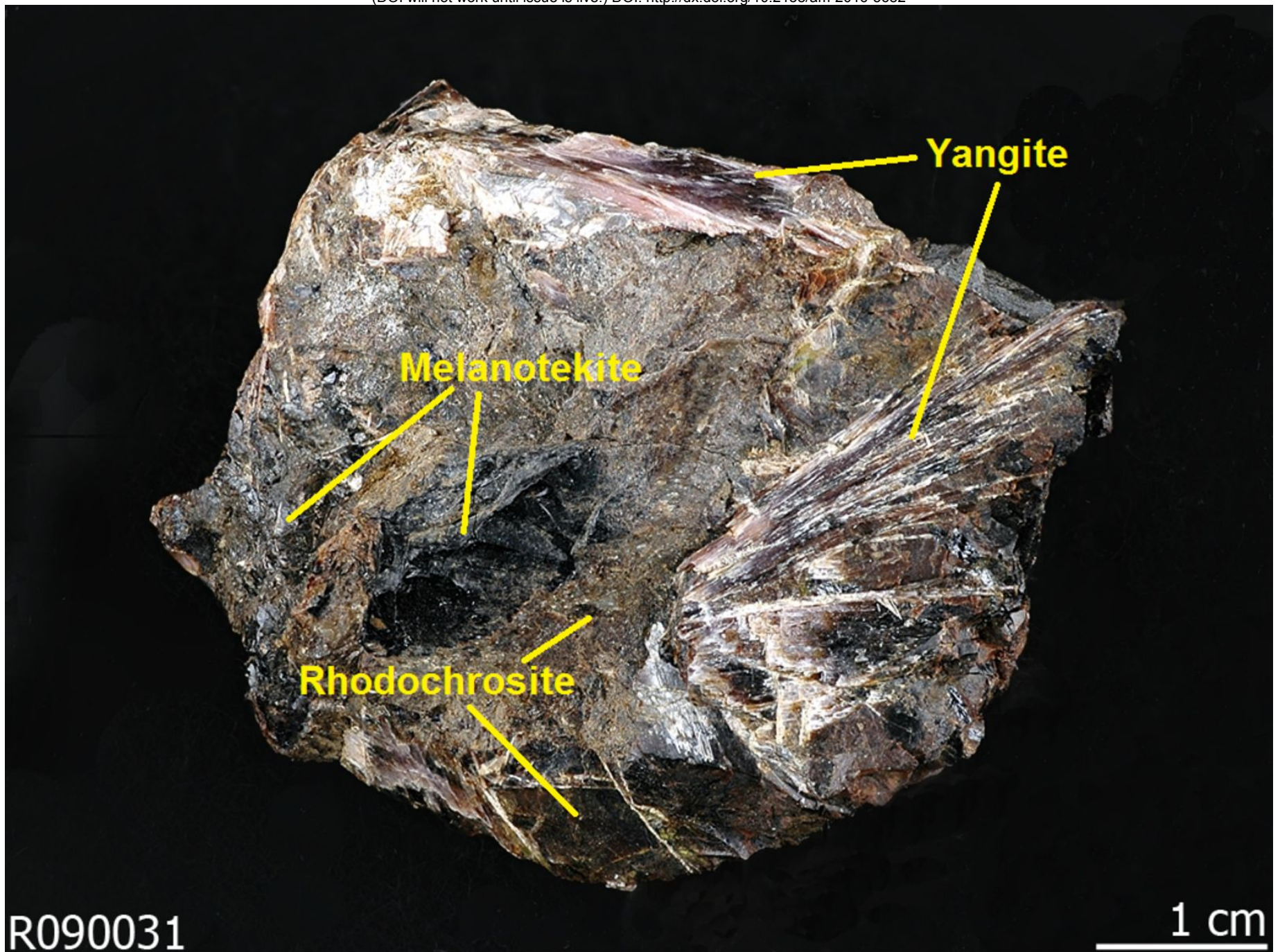


Figure 1a



Figure 1b

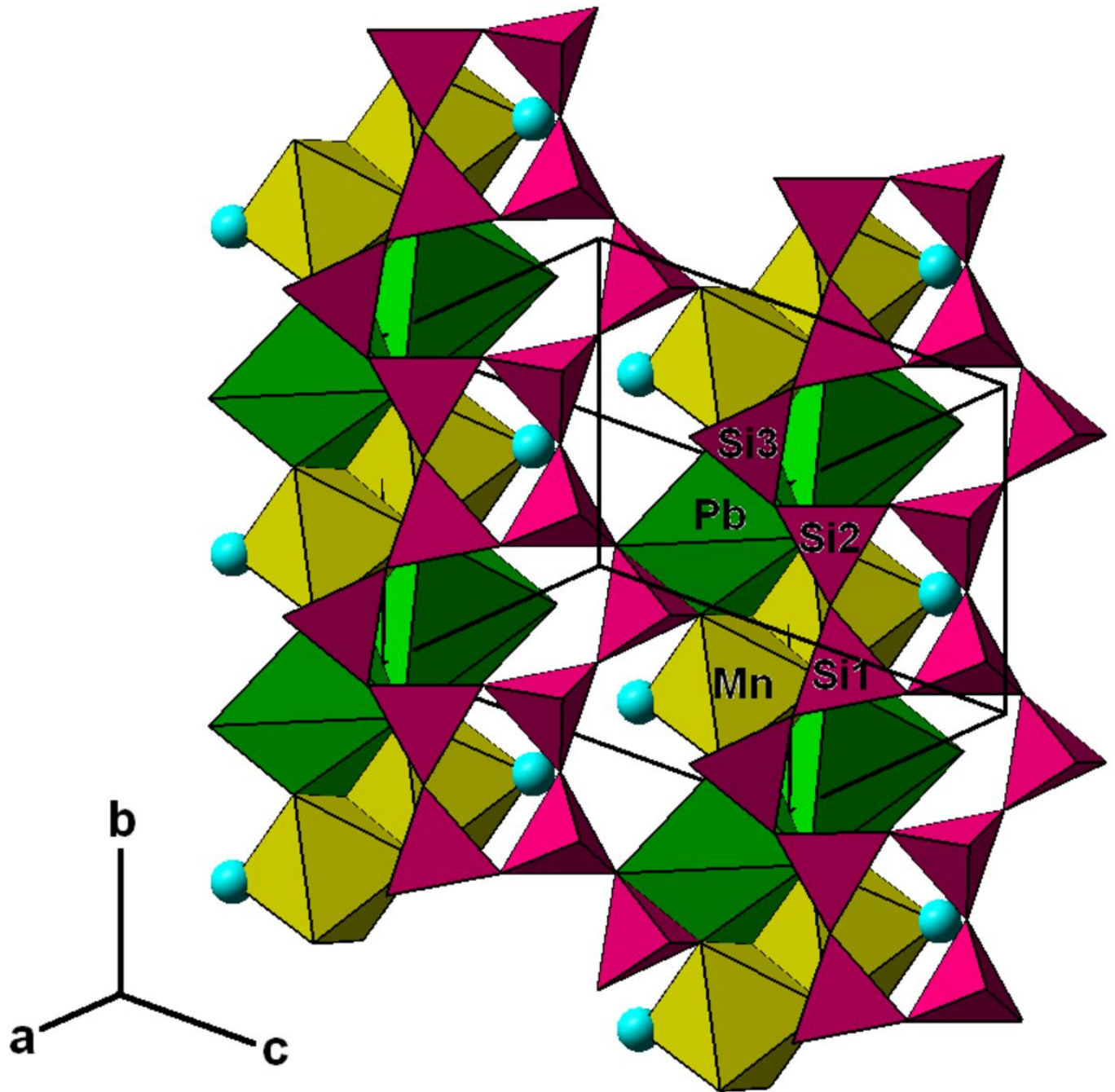


Figure 2a

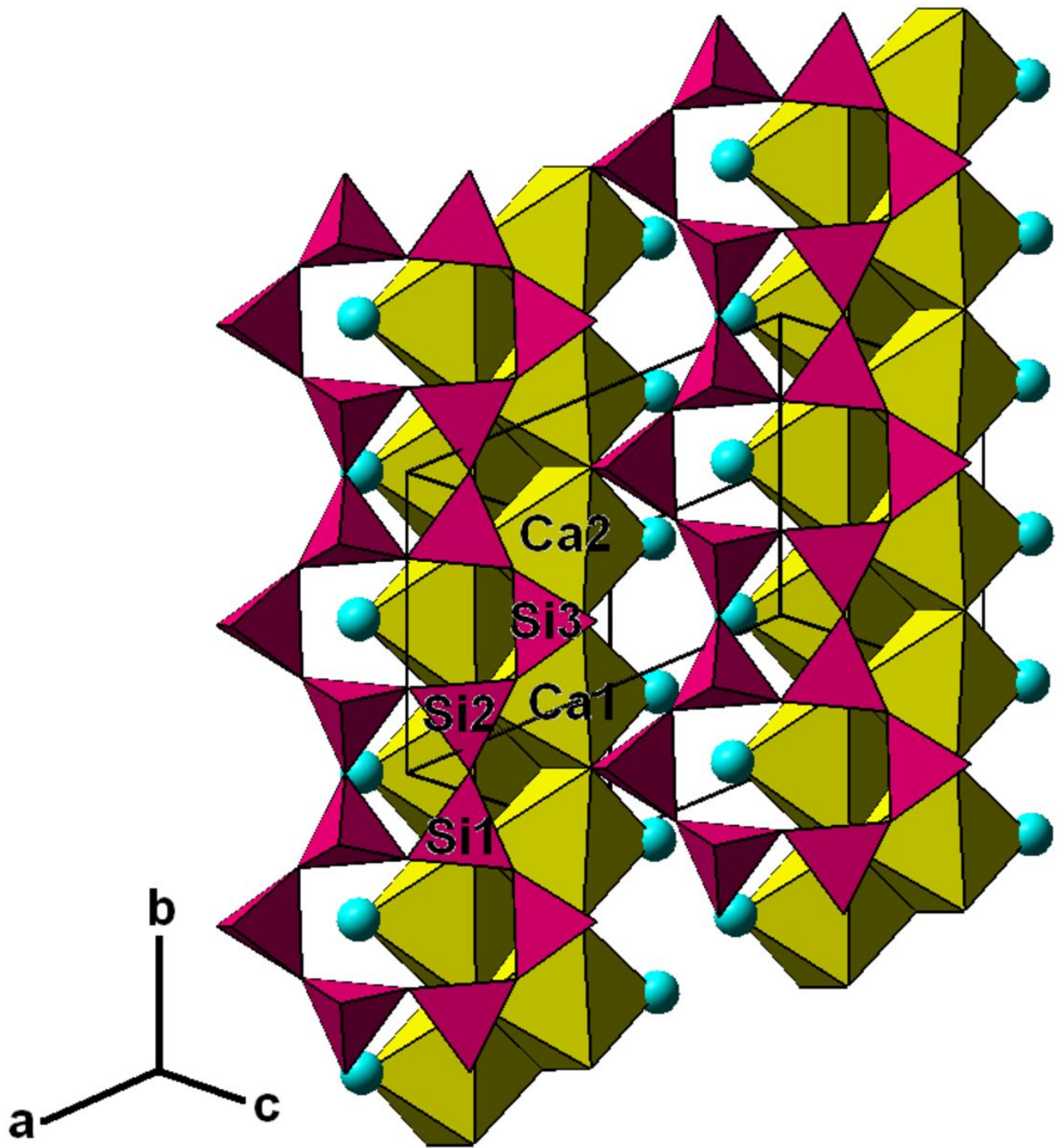


Figure 2b

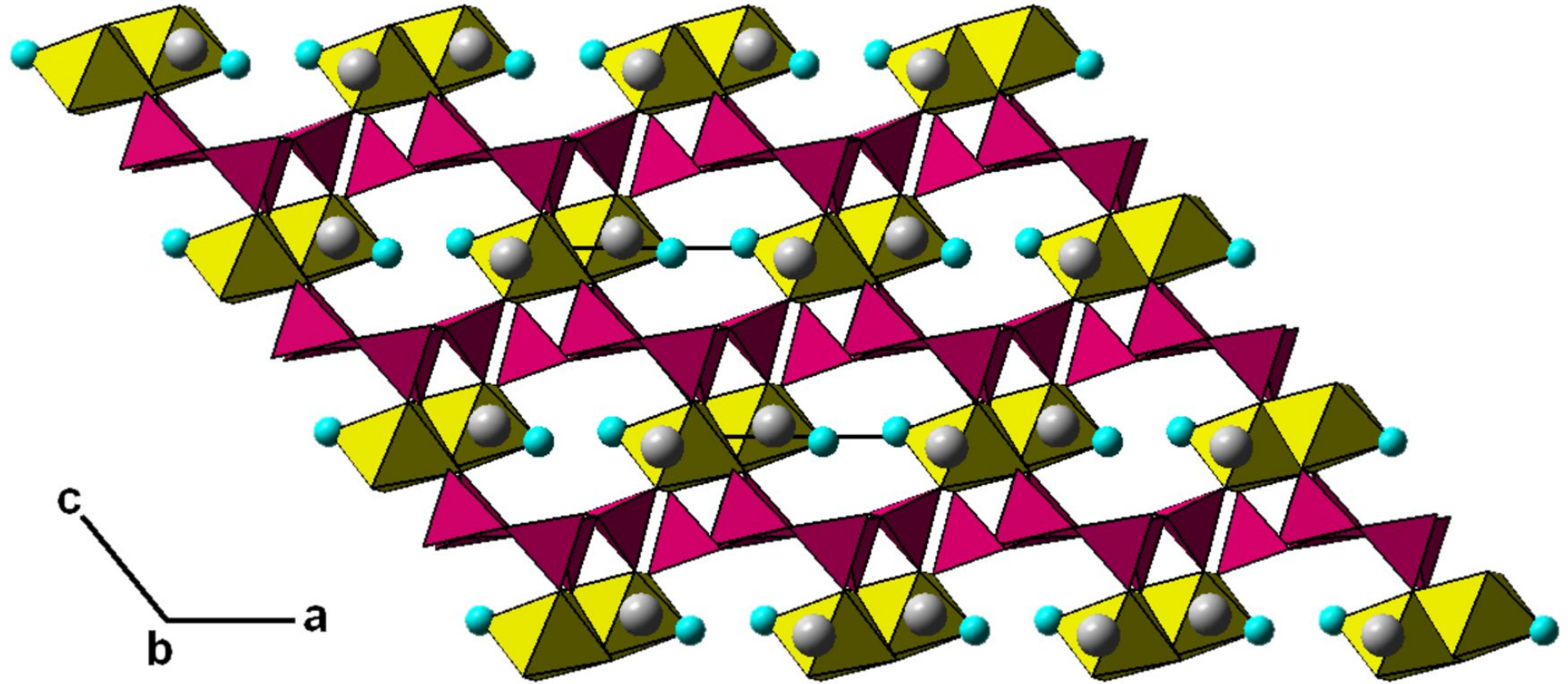


Figure 3

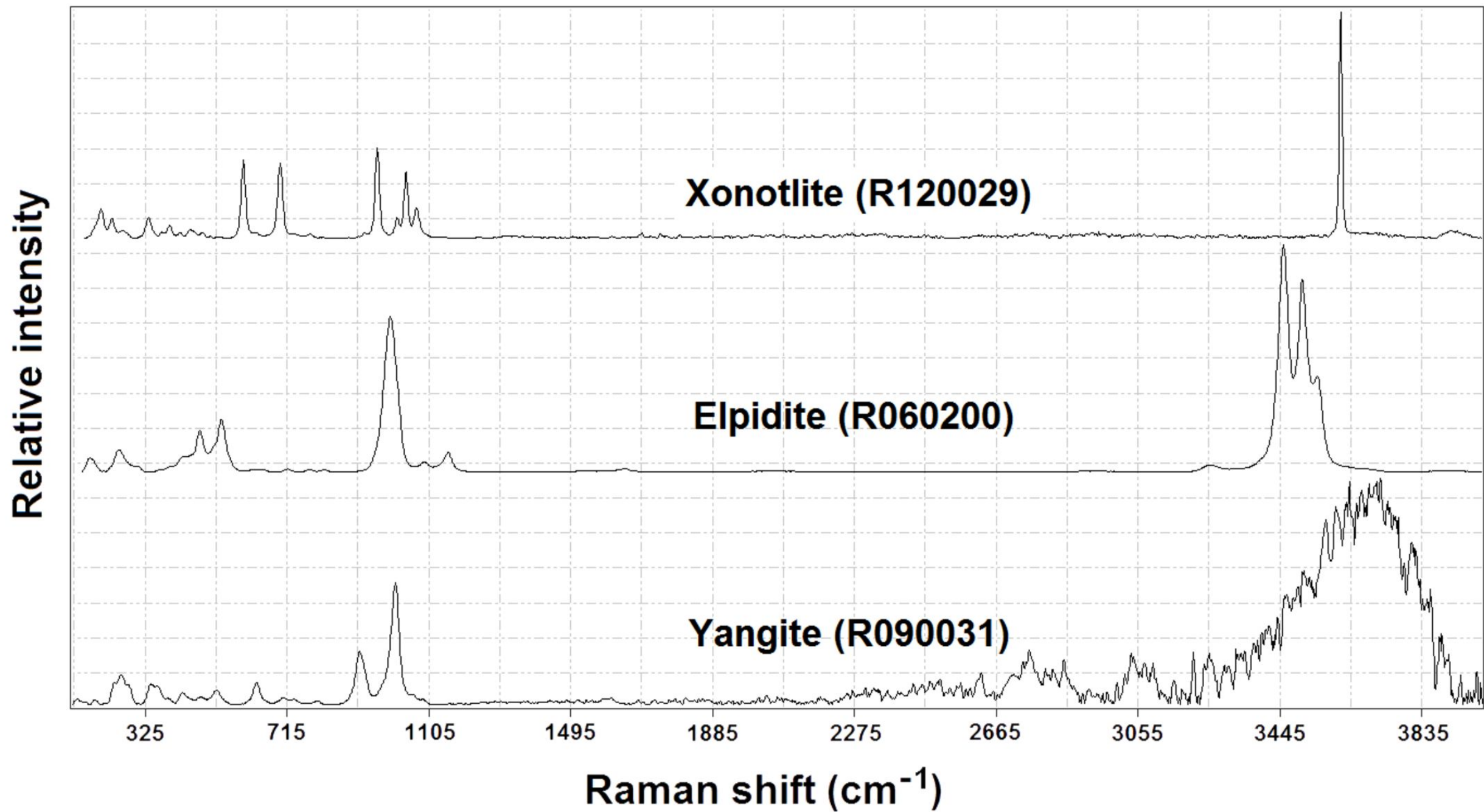


Figure 4

Table 1. Powder X-ray diffraction data for yangite

$I_{\text{meas.}}$	$d_{\text{meas.}}$	$I_{\text{calc.}}$	$d_{\text{calc.}}$	h	k	l
60	7.361	100.00	7.3796	-1	0	1
21	7.023	29.36	7.0353	0	0	1
31	6.671	46.90	6.6489	0	-1	1
30	6.000	31.96	5.9844	1	0	0
10	4.712	13.60	4.7204	-1	1	1
37	4.472	26.68	4.4677	1	-1	1
13	4.272	16.11	4.2765	-1	-1	2
14	3.806	18.74	3.8159	-2	1	1
42	3.697	42.50	3.7173	-2	0	1
		19.73	3.6898	-2	0	2
25	3.591	26.16	3.6054	0	1	1
35	3.514	35.74	3.5177	0	0	2
		9.66	3.5170	-2	1	0
10	3.409	15.52	3.4141	-1	2	0
8	3.321	13.80	3.3244	0	-2	2
18	3.175	24.17	3.1817	-1	-1	3
12	3.111	16.02	3.1177	-1	1	2
53	2.985	35.99	2.9922	2	0	0
100	2.909	60.50	2.9171	1	-2	2
		51.74	2.9076	0	2	0

		27.16	2.8953	-1	-2	2
17	2.761	12.30	2.7678	-1	2	1
15	2.718	7.51	2.7196	-2	-1	1
23	2.447	18.77	2.4378	1	0	2
12	2.390	16.43	2.4003	-3	2	1
6	2.332	4.36	2.3358	-1	-1	4
19	2.275	4.81	2.2775	0	2	1
		5.80	2.2728	-1	-2	4
18	2.220	11.02	2.2338	2	-2	2
18	2.205	13.29	2.1999	1	2	0
9	2.134	8.76	2.1469	1	-1	3
		5.28	2.1348	-3	-1	2
6	2.097	9.08	2.0898	-3	-1	4
9	2.077	4.75	2.0756	-1	0	4
7	2.064	6.60	2.0724	-1	-3	3
4	2.016	11.23	2.0264	3	-2	1
8	1.931	9.46	1.9418	-3	2	3
4	1.856	3.94	1.8478	0	1	3
14	1.805	3.49	1.8027	0	2	2
22	1.783	6.68	1.7939	-3	3	2
		5.28	1.7935	1	-2	4
		4.07	1.7915	2	0	2
10	1.704	5.57	1.7172	3	-2	2
		4.22	1.7118	-1	2	3

15	1.673	7.83	1.6884	2	2	0
13	1.666	4.19	1.6648	3	0	1

=====

Table 2. Crystallographic data and refinement results for yangite

	Yangite	Hypothetical material
Ideal chemical formula	PbMnSi ₃ O ₈ ·2H ₂ O	Ca ₂ Si ₃ O ₈ ·2H ₂ O
Crystal symmetry	Triclinic	Triclinic
Space group	<i>P</i> -1 (#2)	<i>P</i> -1(#2)
<i>a</i> (Å)	9.6015(9)	9.69
<i>b</i> (Å)	7.2712(7)	7.28
<i>c</i> (Å)	7.9833(8)	8.11
α (°)	105.910(4)	103.0
β (°)	118.229(4)	118.5
γ (°)	109.935(5)	112.1
<i>V</i> (Å ³)	392.69(7)	404.30
<i>Z</i>	2	2
ρ_{cal} (g/cm ³)	4.164	
λ (Å, MoK α)	0.71073	
μ (mm ⁻¹)	23.501	
2 θ range for data collection	≤65.58	
No. of reflections collected	9930	
No. of independent reflections	2848	
No. of reflections with $I > 2\sigma(I)$	2460	
No. of parameters refined	128	
R(int)	0.042	
Final R_1 , wR_2 factors [$I > 2\sigma(I)$]	0.031, 0.063	

Final R_1 , wR_2 factors (all data) 0.040, 0.066

Goodness-of-fit 1.00

Reference This work Merlino and Bonaccorsi (2008)

Table 3. Atomic coordinates and displacement parameters for yangite

Atom	x	y	z	Uiso	U11	U22	U33	U23	U13	U12
Pb	0.22536 (3)	0.73792 (3)	0.05494 (3)	0.0132 (1)	0.0134 (1)	0.0145 (1)	0.0143 (1)	0.0075 (1)	0.0098 (1)	0.0084 (1)
Mn	0.1787 (1)	0.2238 (1)	0.0739 (1)	0.0102 (1)	0.0091 (3)	0.0102 (3)	0.0112 (3)	0.0056 (3)	0.0060 (3)	0.0057 (3)
Si1	0.1178 (2)	0.2686 (2)	0.4471 (2)	0.0080 (2)	0.0078 (6)	0.0080 (6)	0.0084 (6)	0.0046 (5)	0.0049 (5)	0.0046 (5)
Si2	0.1430 (2)	0.8580 (2)	0.4314 (2)	0.0086 (2)	0.0089 (6)	0.0096 (6)	0.0098 (6)	0.0058 (5)	0.0062 (5)	0.0063 (5)
Si3	0.4104 (2)	0.7099 (2)	0.5425 (2)	0.0087 (2)	0.0061 (6)	0.0075 (6)	0.0095 (6)	0.0041 (5)	0.0035 (5)	0.0037 (5)
O1	0.0058 (5)	0.1535 (6)	0.1840 (6)	0.0107 (6)	0.010 (2)	0.013 (2)	0.009 (2)	0.006 (1)	0.005 (1)	0.006 (1)
O2	0.3099 (5)	0.5233 (6)	0.5936 (6)	0.0105 (6)	0.009 (2)	0.007 (2)	0.010 (2)	0.004 (1)	0.004 (1)	0.002 (1)
O3	0.1868 (5)	0.1149 (6)	0.5347 (6)	0.0101 (6)	0.012 (2)	0.010 (2)	0.011 (2)	0.007 (1)	0.007 (1)	0.008 (1)
O4	-0.0103 (5)	0.2891 (6)	0.5213 (6)	0.0135 (7)	0.017 (2)	0.013 (2)	0.021 (2)	0.012 (1)	0.015 (2)	0.011 (1)
O5	0.3482 (5)	0.8942 (6)	0.5801 (6)	0.0122 (7)	0.011 (2)	0.011 (2)	0.014 (2)	0.006 (1)	0.006 (1)	0.009 (1)
O6	0.0403 (5)	0.7286 (6)	0.1679 (6)	0.0112 (7)	0.012 (2)	0.013 (2)	0.009 (2)	0.006 (1)	0.007 (1)	0.007 (1)
O7	0.3252 (5)	0.5838 (6)	0.2877 (6)	0.0129 (7)	0.015 (2)	0.012 (2)	0.012 (2)	0.006 (1)	0.008 (1)	0.008 (1)
O8	0.6363 (5)	0.8585 (6)	0.7301 (6)	0.0110 (7)	0.008 (2)	0.011 (2)	0.015 (2)	0.007 (1)	0.006 (1)	0.005 (1)
O9W	0.3552 (6)	0.3169 (9)	0.9730 (7)	0.033 (1)	0.016 (2)	0.051 (3)	0.018 (2)	0.013 (2)	0.011 (2)	0.009 (2)

Table 4. Selected bond distances in yangite

	Distance (Å)		Distance (Å)		Distance (Å)
Si1-O1	1.599(3)	Si2-O3	1.624(3)	Si3-O2	1.650(3)
-O2	1.626(4)	-O4	1.630(4)	-O5	1.655(3)
-O3	1.635(3)	-O5	1.619(3)	-O7	1.594(4)
-O4	1.629(3)	-O6	1.613(4)	-O8	1.599(4)
Ave.	1.622		1.622		1.624
TAV	13.73		11.24		20.95
TQE	1.0031		1.0027		1.0049
Pb-O1	2.684(3)	Mn-O1	2.200(3)		
-O6	2.333(3)	-O1	2.245(3)		
-O6	2.770(3)	-O6	2.300(3)		
-O7	2.412(3)	-O7	2.124(3)		
-O8	2.397(3)	-O8	2.138(3)		
-O5	3.063(3)	-O9w	2.188(4)		
Ave.	2.610	Ave.	2.199		
		OAV	34.06		
		OQE	1.0104		

Note: TAV---tetrahedral angle variance; TQE---tetrahedral quadratic elongation OAV---
octahedral angle variance; OQE---octahedral quadratic elongation (Robinson et al. 1971).

Table 5. Calculated bond-valence sums for yangite.

	O1	O2	O3	O4	O5	O6	O7	O8	O9w	Sum
Pb	0.21			0.02	0.03	0.55	0.44	0.46	0.01	1.95
					0.06	0.17				
Mn	0.33					0.25	0.40	0.39	0.35	2.01
	0.29									
Si1	1.07	1.00	0.98	0.99						4.04
Si2			0.99	0.98	1.01	1.03				4.01
Si3		0.93			0.92		1.09	1.07		4.01
Sum	1.90	1.93	1.97	1.99	2.02	2.00	1.93	1.92	0.36	

Note: The parameters used for the calculations were from Brese and O'Keeffe (1991).